

ARTICLE OPEN



CirCHAS2 promotes the proliferation, migration, and invasion of gastric cancer cells by regulating PPM1E mediated by hsa-miR-944

Shuo Ma^{1,2,3,5}, Xinliang Gu^{1,2,3,5}, Lei Shen^{1,2,3}, Yin hao Chen^{1,2,4}, Chen Qian¹, Xianjuan Shen²✉ and Shaoqing Ju¹✉

© The Author(s) 2021

Gastric cancer (GC) is considered one of the most common gastrointestinal malignancies worldwide. Circular RNAs (circRNAs) are a new class of endogenous noncoding RNAs, which can be used as biomarkers and therapeutic targets for many tumors. However, the role and potential regulatory mechanisms of circRNAs in GC remain unclear. In this study, we demonstrated that a specific circRNA, cirCHAS2, was upregulated in GC tissues and cells and was positively correlated with tumor metastasis. In vitro experiments demonstrated that cirCHAS2 knockdown or the addition of hsa-miR-944 mimics inhibited the proliferation, migration, and invasion ability of GC cells and affected the epithelial-mesenchymal transition. In addition, hsa-miR-944 interacted with protein phosphatase, Mg²⁺/Mn²⁺-dependent 1E (PPM1E), and was found to be a target gene of cirCHAS2. The upregulation of PPM1E reversed the effects of cirCHAS2 knockout on GC cells. The cirCHAS2/hsa-miR-944/PPM1E axis may be involved in the progression of GC; thus, cirCHAS2 may be a potential biomarker and therapeutic target for GC.

Cell Death and Disease (2021)12:863; <https://doi.org/10.1038/s41419-021-04158-w>

INTRODUCTION

Gastric cancer (GC) is considered to be one of the most common gastrointestinal malignancies, and its mortality rate ranks third worldwide [1, 2]. GC can be caused by many factors including *Helicobacter pylori* infection, precancerous lesions, diet, or genetic factors [3, 4]. It tends to spread through the lymph nodes to neighboring tissues or organs and produces more cancer cells in the bloodstream [5]. Although significant progress has been made in the diagnosis and treatment of GC in recent years, the overall survival (OS) of GC patients is still unsatisfactory, with a 5-year OS rate of less than 30% [6]. Therefore, it is urgent to identify effective biomarkers and understand their roles in the occurrence and development of GC.

Circular RNAs (circRNAs) are a special type of endogenous small RNAs, which are widely distributed and diverse [7]. They are formed by back-splicing to produce a covalently closed circular structure, usually by the cyclization of exons [8, 9]. Although Sanger et al. discovered the circRNA molecule as early as 1976, after more than 40 years of development, the biological functions of circRNAs are still largely unclear [10, 11]. CircRNAs are widely distributed in eukaryotic cells, have long half-lives, and are expressed at tissue- and stage-specific levels [12]. They can be used as a biomarker and therapeutic target for many tumors. For example, Ding et al. [13] found that circ-DONSON promoted the progression of GC by activating the expression of SRY-box transcription factor four via recruitment of the nucleosome remodeling factor complex.

Fan et al. [14] found that circNR3C2 can act as a potential prognostic biomarker in breast cancer and negatively modulate breast cancer metastasis through the NR3C2/miR-513a-3p/Hrd1/vimentin axis. In recent years, studies have shown that circRNAs can encode regulatory proteins/peptides in unique ways [15–17]. However, owing to the small number of circRNAs that can encode, the encoding mechanism has not been effectively explained. The mainstream understanding of circRNAs as a molecular regulatory mechanism in diseases is that they function as a microRNA (miRNA) sponge to regulate tumor proliferation, metastasis, drug resistance, and other functions [18–20]. For example, circCUL2 regulates the expression of Rho-associated coiled-coil containing protein kinase two by regulating miR-142-3p, and regulates the tumor progression of GC by activating the autophagy pathway [21]. CircUBAP2 regulates the malignant behavior of osteosarcoma cells through the miR-204-3p/HMGA2 axis [22]. CircAGAP1 promotes the development of renal clear cell carcinoma by binding with miR-15-5p to promote E2F transcription factor 3 expression [23]. Recent studies have shown that circRNAs play a critical role in the genesis and development of GC [24, 25]. The mechanism of circRNA as a competing endogenous RNA (ceRNA) in GC has not been fully explored, and its physiological and pathological roles in GC are not completely understood.

In this study, we identified a novel circRNA, cirCHAS2. We confirmed that cirCHAS2 can competitively bind with hsa-miR-944 to affect the expression of PPM1E in GC and ultimately act as a

¹Department of Laboratory Medicine, Affiliated Hospital of Nantong University, Nantong 226001 Jiangsu, China. ²Research Center of Clinical Medicine, Affiliated Hospital of Nantong University, Nantong 226001 Jiangsu, China. ³Medical School of Nantong University, Nantong University, Nantong 226001 Jiangsu, China. ⁴Department of Urology, Affiliated Hospital of Nantong University, Nantong 226001 Jiangsu, China. ⁵These authors contributed equally: Shuo Ma, Xinliang Gu. ✉email: juanxia819@163.com; jsq814@hotmail.com
Edited by Professor Roberto Mantovani

Received: 30 April 2021 Revised: 19 August 2021 Accepted: 9 September 2021

Published online: 23 September 2021

tumor promoter. Thus, circHAS2 may serve as a potential biomarker and therapeutic target for GC.

METHODS

Clinical samples

A total of 60 pairs of gastric and paracancerous tissues were collected from the Department of Pathology, Affiliated Hospital of Nantong University (Jiangsu, China). All of the specimens were immediately frozen in -80°C liquid nitrogen after resection, and total RNA was extracted. All of the specimens were pathologically diagnosed as GC. Tissues were collected from August 2016 to October 2021. The study was approved by the local ethics committee (ethical review report number: 2018-L055). Patients did not receive radiotherapy or chemotherapy before surgery. All of the GC patients and healthy control participants consented to the clinical trial and publication of the article.

RNA extraction and quantitative PCR

Total RNA from GC tissues and cells was extracted using TRIzol reagent (Invitrogen, Ontario, Canada). Total RNA was reverse transcribed into cDNA at 42°C for 10 min and at 72°C for 1 h using a reverse transcription kit (Thermo Fisher Scientific, Waltham, MA, USA). The Roche LightCycler 480 (Roche, Switzerland) was used for quantitative PCR (qPCR) (20- μL total volume; denaturation 95°C , 10 s; annealing 60°C , 30 s; 45 cycles. GAPDH rRNA was used as an internal reference for circHAS2, HAS2, and PPM1E, and U6 rRNA was used as an internal reference for hsa-miR-944. The primer sequences were circHAS2 (forward-5'-TGTACAGATGCATTGTGAGAG-3') and (reverse-5'-GCTGTGATTCCAAGGAG-3'); HAS2 (forward-5'-CCTCATCATCCAAAGCCTGT-3') and (reverse-5'-GATGCAAAGGGCAACTGTTT-3'); PPM1E (forward-5'-GCTTTAGCCAGAGCCACATC-3') and (reverse-5'-ACAGTCCCTCTGTGCCATC-3'); GAPDH (forward-5'-TCCCATCACCATCTCCAGG-3') and (reverse-5'-GATGACCCCTTTGGCTCCC-3'); U6 (forward-5'-AACGCTTACGAAATTTGCGT-3') and (reverse-5'-CTCGCTCGGCAGCACA-3').

The hsa-miR-944 primer sequence was obtained from RiboBio Co., Ltd. (Guangzhou, China). The $2^{-\Delta\Delta\text{CT}}$ method was used to calculate the relative expression levels of plasma circRNAs.

Cell culture

We obtained GC cells (AGS, MKN-1, HGC-27, MKN-45, SGC-7901, MGC-803, BGC-823) and gastric epithelial cells (GES-1) from the Chinese Academy of Sciences (Shanghai, China). All of the cells were cultured in RPMI-1640 medium (Corning, New York, NY, USA) supplemented with 10% fetal bovine serum (FBS) (Gibco, Gaithersburg, MD, USA) and 1% penicillin and streptomycin (Newcells Biotech Co., Ltd., Tyne UK). The culture condition was 37°C , 5% carbon dioxide. The media were changed every 3 days.

RNase R and actinomycin D assay

According to the amount of RNA, RNase R (Geneseed, Guangzhou, China) was used for treatment, and cells were incubated at 37°C for 20 min. After treatment, the expression of circHAS2 and HAS2 in the cells was detected by qPCR. The cells were cultured in medium containing actinomycin D (blocks RNA transcription) for 0, 2, 4, 8, 12, and 24 h, and then the RNA was detected by qPCR.

Plasmid construction and transfection

After the cells were grown to 60–70% confluency, they were transfected with short hairpin negative control (shNC), shRNA1, shRNA2, shHAS2-1, shHAS-2, mimics NC, hsa-miR-944 mimics, OE-NC, and OE-PPM1E using Lipofectamine 3000 (Thermo Fisher Scientific) and harvested after 24–48 h.

Cell counting Kit-8 assay

Cells transfected for 24–48 h were collected and counted. The cell suspension was diluted to $3 \times 10^4/\text{mL}$ and plated in 96-well plates. Cells were incubated for 24, 48, 72, 96, or 120 h with four replicates for each timepoint. Then, 10 μL CCK-8 reagent (Dojindo, Kumamoto, Japan) was added to each well at the corresponding timepoint. A microplate analyzer measured the absorbance of each well at 450 and 630 nm at 2 h.

Colony formation assay

Cells were collected at 24–48 h after transfection, and 1000 cells per well were seeded in 6-well plates. The culture medium was changed every

4 days, and after 2 weeks of culture, cells were fixed in paraformaldehyde for 12–24 h, stained with crystal violet, and photographed.

Transwell assay

Cells transfected for 24–48 h were collected, and the cell density was adjusted to $5 \times 10^5/\text{mL}$ for the cell migration experiment and $8 \times 10^5/\text{mL}$ for the cell invasion experiment. Then 500- μL RPMI-1640 medium was added to the 24-well plates. Then the transwell inserts were added to the plates. In the invasion experiment, Matrigel (Corning) and RPMI-1640 medium were mixed at a ratio of 1:6 and added to the upper chamber. The cell suspension was added to the chamber and removed after 48 h, fixed in paraformaldehyde, stained with crystal violet, and photographed under a microscope.

5-Ethynyl-2'-deoxyuridine assay

Cells were evenly seeded into 24-well plates at a density of 1×10^5 cells per well. The EdU Kit (RiboBio) was used to detect proliferating cells. After the cells adhered to the wall, the culture medium was changed to medium containing 50 μM EdU and incubated for 2 h. Then the cells were stained with Apollo and Hoechst 33342. The cells were observed by fluorescence microscopy. The EdU-positive cell rate (the ratio of EdU-positive cells to the total number of DAPI-stained cells) was calculated.

Fluorescence in situ hybridization

The cells were evenly inoculated in a 24-well plate. After the cells adhered to the wall, the cells were washed with phosphate-buffered saline and fixed in paraformaldehyde for 30 min. Then a permeability solution was added for permeability. A hybrid solution containing circHAS2 and 18 S and a U6 probe (RiboBio) was added to each well overnight. Then cells were washed three times with lotion containing SSC (Sangon Biotech, Shanghai, China). Then nuclear staining was performed with Hoechst 33342 (RiboBio) or DAPI, followed by fluorescence microscopy.

Dual-luciferase reporter assay

CircHAS2 and PPM1E sequences containing wild-type (WT) and mutant (MUT) hsa-miR-944 binding sites were synthesized and inserted into a luciferase vector (RiboBio), which was co-transfected into GC cells with hsa-miR-944 mimics. After transfection for 48 h, the cells were lysed. A dual-luciferase assay kit (Vazyme Biotech Co., Ltd., Nanjing, China) was used to detect luciferase activity.

Western blot analysis

After transfection for 48 h, the cells were lysed in RIPA buffer with PMSF (SolarBio Life Science, Beijing, China). The proteins were resolved by sodium dodecyl sulfate-polyacrylamide gel electrophoresis and electrotransferred to a polyvinylidene fluoride membrane (Millipore, Billerica, MA, USA). The membrane was blocked in a rapid blocking solution (Shanghai EpiZyme Biotechnology, Shanghai, China) and then incubated with primary antibodies overnight at 4°C . Next, the membrane was washed 2–3 times with Tris-buffered saline with 0.1% Tween[®] 20 detergent (TBST), followed by incubation with horseradish-peroxidase (HRP)-labeled secondary antibodies (Cell Signaling Technology, Danvers, MA, USA) at room temperature for 2 h and then another 2–3 washes with TBST. Finally, proteins were visualized by enhanced chemiluminescence (Vazyme Biotech Co., Ltd., Nanjing, China).

RNA immunoprecipitation assay

The BersinBio[™] RNA Immunoprecipitation (RIP) Kit (BersinBio, Guangzhou, China) was used to perform the RIP experiments. HGC-27 and MKN-45 cells overexpressing hsa-miR-944 were used. Cells were lysed in RNA lysis buffer and then incubated at 4°C overnight with RIP buffer containing coupled Argonaute-2 (AGO2) antibody (Proteintech, Rosemont, IL, USA) or negative control IgG. Then the magnetic beads were washed three times. After proteinase K treatment, the immunoprecipitated RNA was extracted with phenol-chloroform-isopentyl alcohol (25:24:1). Finally, qPCR was used to detect the expression of circHAS2 and hsa-miR-944.

Bioinformatics analyses

Cross-analysis of the prediction databases circAtlas (<http://circatlas.biols.ac.cn/>), Starbase (<http://starbase.sysu.edu.cn/>), CircBank (<http://www.circbank.cn/index.html>), and Circinteractome (<http://circinteractome.nia.nih.gov/>)

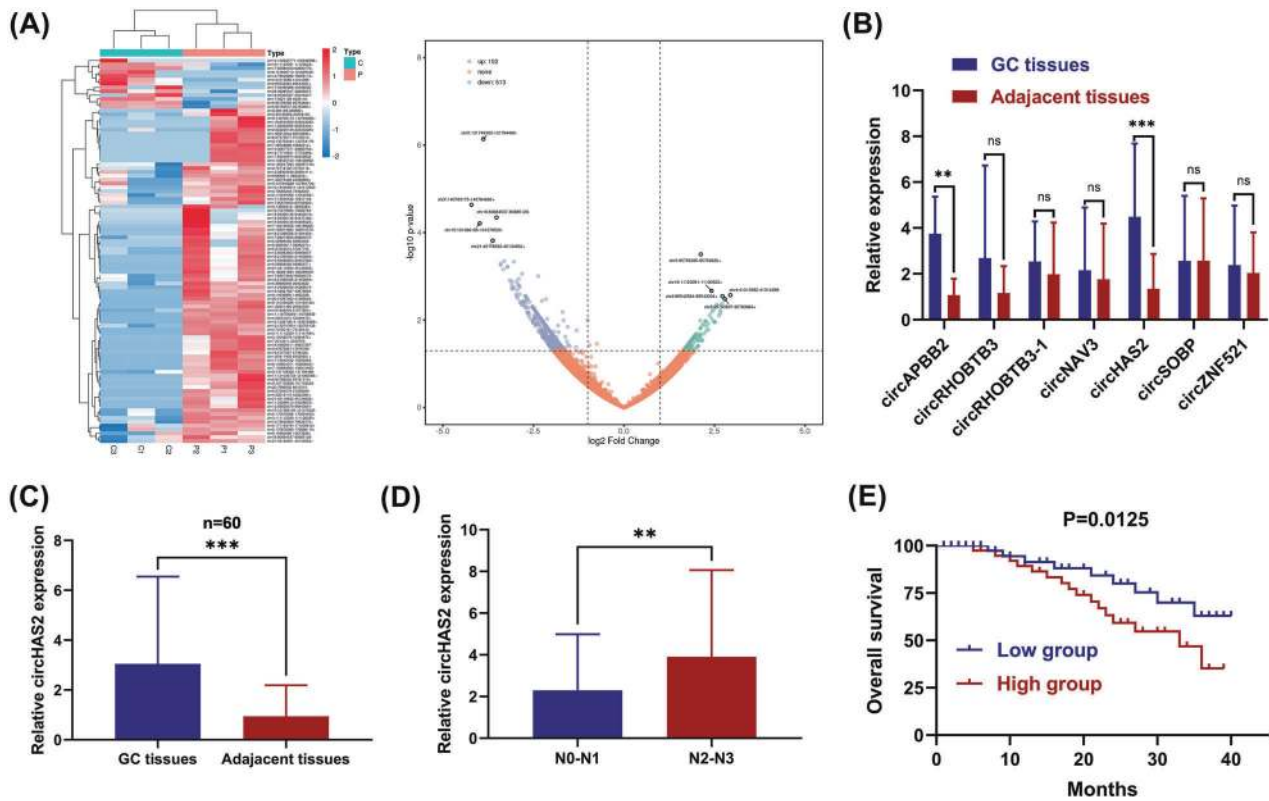


Fig. 1 Identification and screening of circHAS2. **A** Heat map and volcano map analysis were performed for circRNAs differentially expressed in GC tissues and corresponding paracancerous tissues in three pairs of GSE121445. **B** The expression level of circRNAs differentially expressed in 7 databases in 20 pairs of GC tissues and paracancerous tissues was detected by qPCR. **C** The expression level of circHAS2 in 60 pairs of GC tissues and corresponding paracancerous tissues. **D** The expression level of circHAS2 at different N stages in GC. **E** The prognostic value of circHAS2 by survival curve analysis. ** $P < 0.01$, *** $P < 0.001$.

was conducted. The target gene circHAS2 was obtained by the cross-analysis of four databases. Moreover, the MiRDB (<http://mirdb.org/index.html>), MiRWalk (<http://mirwalk.umm.uni-heidelberg.de/>), MiRPathDB (<https://mpd.bioinf.uni-sb.de/overview.html>), and Targetscan (http://www.targetscan.org/vert_72/) databases were used for the intersection and cross-analysis of target genes of hsa-miR-944.

Statistical analyses

SPSS16.0 software (SPSS, Chicago, IL, USA) and GraphPad Prism version 8.0 (GraphPad Software, La Jolla, CA, USA) were used for statistical analyses. All of the experiments were conducted in triplicate, and all of the data are expressed as the mean \pm standard deviation. Student's *t* test or one-way analysis of variance evaluated the differences between two or more groups. The relationship between circHAS2 and linear HAS2 or hsa-miR-944 was evaluated using Pearson's correlation coefficient. Survival was analyzed using the Kaplan–Meier survival curve. $P < 0.05$ was considered to be statistically significant.

RESULTS

CircHAS2 is upregulated in GC and is associated with GC progression

To investigate the biological function of circRNAs in GC, we analyzed the differentially expressed circRNAs in three pairs of GC tissues and corresponding paracancerous tissues from GSE121445 data. A total of 615 circRNAs were differentially expressed in the database, including 102 upregulated and 513 downregulated (Fig. 1A). We selected seven circRNAs (circAPBB2, circRHOBTB3, circRHOBTB3-1, circNAV3, circHAS2, circSOBP, and circZNF521) with the highest upregulated expression meeting the criteria of fold change >2 and $P < 0.05$. Their relevant information is shown in Supplementary Table 1. Subsequently, qPCR was used to verify the differences in expression levels of these seven upregulated

circRNAs in 20 pairs of GC tissues and their corresponding paracancerous tissues. The results showed that only circAPBB2 and circHAS2 were significantly upregulated, and the upregulation of circHAS2 was the most significant (Fig. 1B). Then qPCR was used to further analyze the expression of circHAS2 in 60 pairs of GC tissues and corresponding paracancerous tissues, and the expression of circHAS2 in GC tissues was significantly higher than that in normal paracancerous tissues (Fig. 1C). According to different lymph node metastasis cases in GC tissues, the expression level of circHAS2 was found to increase with the increase in lymph node metastasis (Fig. 1D). In addition, the GC group was divided into a high expression group (expression level >3.0524) and low expression group (expression level ≤ 3.0524) based on the median expression level of GC tissue as the limit. After analyses of the clinical data, it was found that the expression of circHAS2 was correlated with T stage, tumor-node-metastasis (TNM) stage, lymph node metastasis, and nerve/vascular invasion but not with other characteristics (Table 1). After comparing survival curves, it was found that the survival status of the low expression group was significantly better than that of the high expression group (Fig. 1E). These results indicated that the expression of circHAS2 was upregulated in GC and correlated with the metastasis and prognosis of GC.

Characteristics and basic information of circHAS2

The circBase database (<http://www.circbase.org/>) and UCSC database (GRCh37/hg19) (<http://genome.ucsc.edu/>) showed that circHAS2 was located at chr8:122,640,953–122,641,580, with a mature transcript length of 627 base pairs (bp), which was formed by cyclization of exon 2 (Fig. 2A). In addition, we designed divergent primers for reverse amplification of circHAS2 based on the cyclization site of circHAS2. The qPCR products were detected

Table 1. Clinical Bentley analysis of circHAS2.

Parameter		No. of patients	circHAS2(high)	circHAS2(low)	P value
Sex	male	32	18	14	0.536
	female	28	16	12	
Age (year)	<60	15	9	9	0.319
	≥60	45	27	18	
Tumor size	<5	43	28	15	0.074
	≥5	17	10	7	
Differentiation grade	Well-moderate	19	10	9	0.106
	Poor-undifferentiation	41	20	21	
T stage	T1-T2	35	21	14	0.0351*
	T3-T4	25	14	11	
Lymph node status	Positive	39	24	15	0.001***
	Negative	21	16	5	
TNM stage	I-II	51	35	16	<0.0001****
	III-IV	9	7	2	
Nerve/vascular invasion	Positive	33	19	14	0.0125**
	Negative	27	19	8	

* $P < 0.05$, ** $P < 0.01$, *** $P < 0.001$, **** $P < 0.0001$.

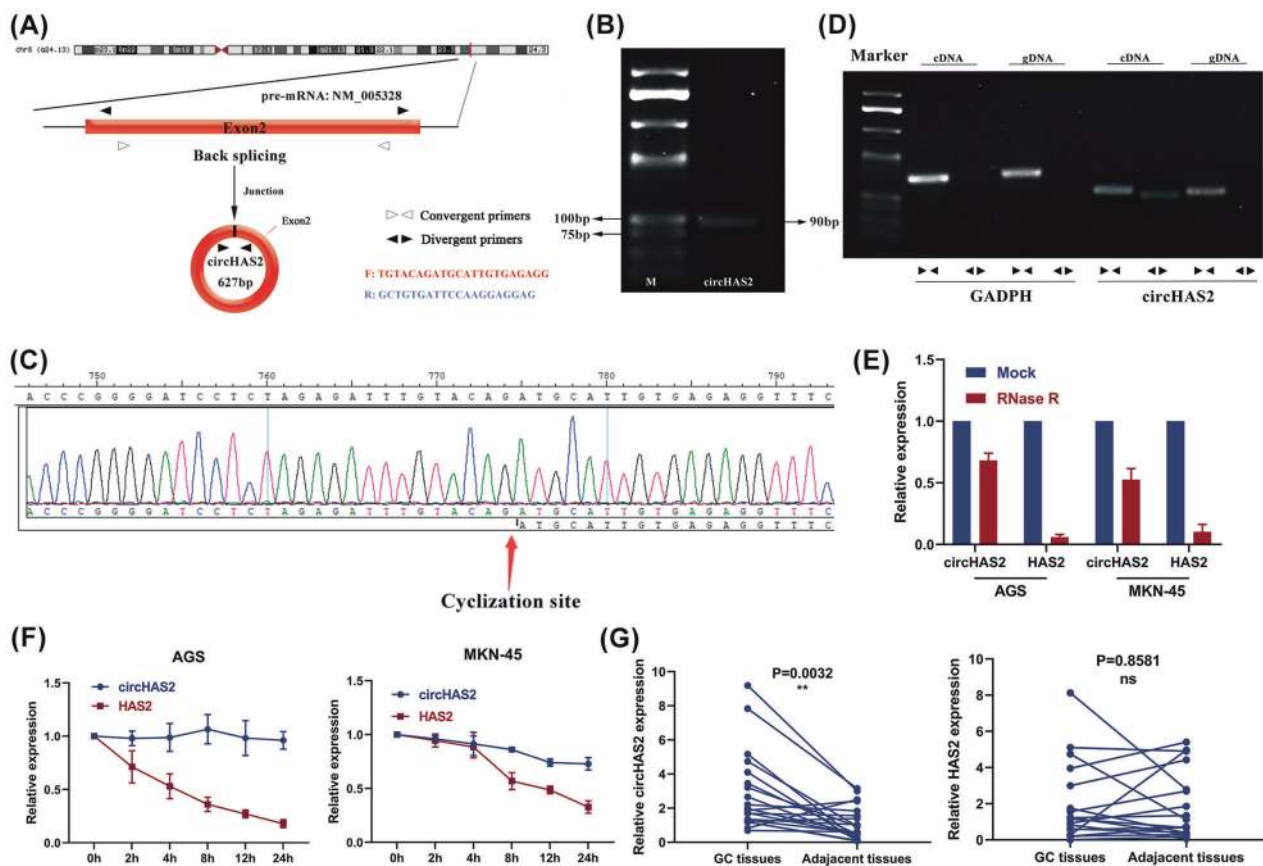


Fig. 2 Basic information and characteristics of circHAS2. **A** Schematic diagram of chromosomal location and formation of circHAS2. **B** and **C** Agarose gel electrophoresis and Sanger sequencing verified the primer length and cyclization site of circHAS2. **D** Verify the circular structure of circHAS2. **E** and **F** RNase R and actinomycin D were used to verify the stability of circHAS2. **G** The expression levels of circHAS2 and HAS2 were detected by qPCR. ** $P < 0.01$.

by 2.5% agarose gel electrophoresis, and the band length was 90 bp, consistent with the size of the primer products (Fig. 2B). In addition, Sanger sequencing further confirmed the reverse splicing site of circHAS2 (Fig. 2C). After agarose gel electrophoresis

of qPCR products of genomic DNA and cDNA, it was found that the reverse amplification products of circHAS2 only appeared in cDNA, and the circular structure of circHAS2 was also verified by the above experiments (Fig. 2D). We treated AGS and MKN-45 cells

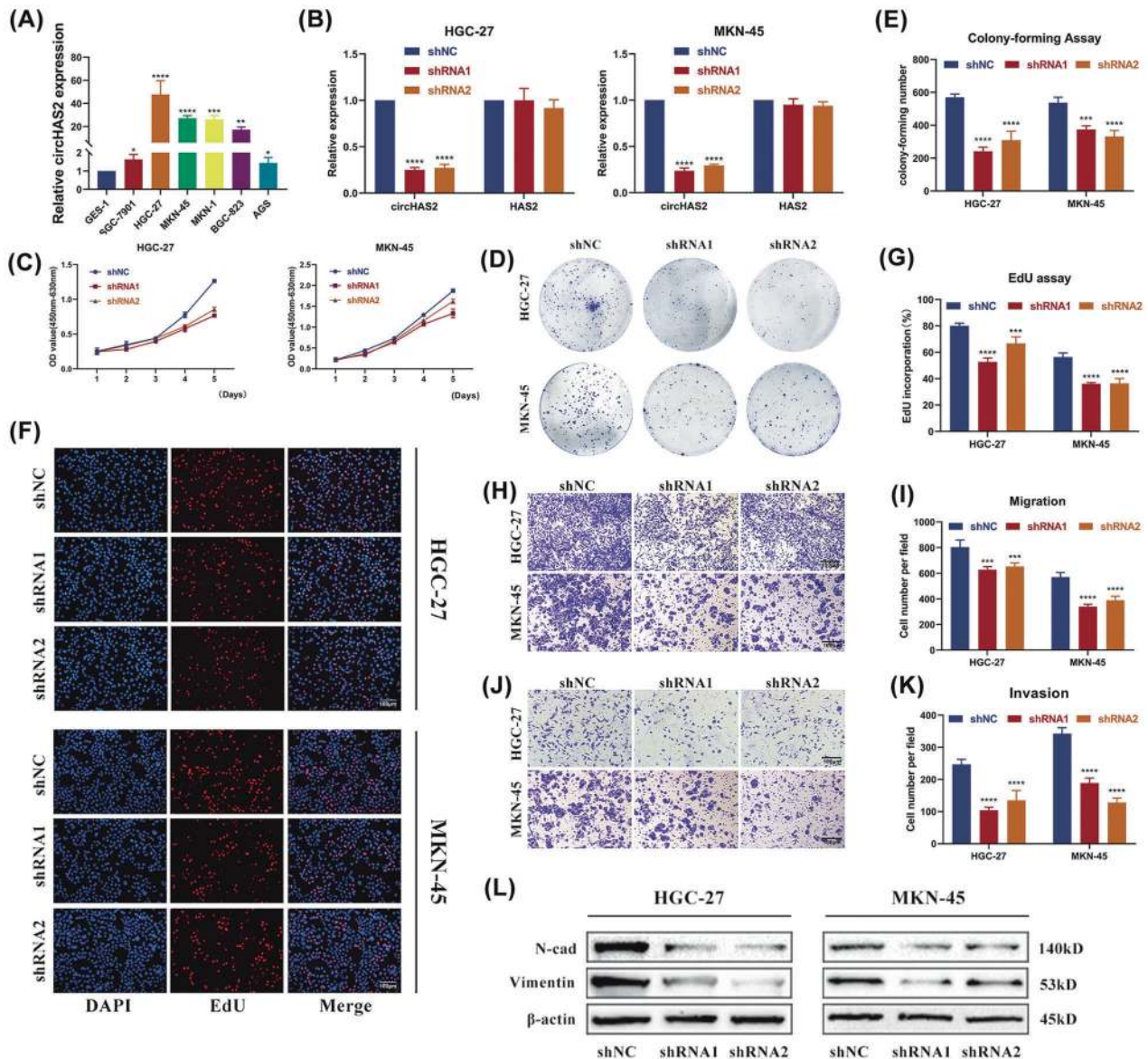


Fig. 3 circHAS2 can promote the proliferation, migration, and invasion of GC cells. **A** The expression level of circHAS2 in GC cells. **B** Knocking efficiency of GC cells transfected with plasmids shNC, shRNA1, and shRNA2. **C–G** The effects of circHAS2 knockdown on the proliferation ability of HGC-27 and MKN-45 cells were evaluated by CCK-8, cell colony formation assay, and EdU assay. **H–K** The effects of circHAS2 knockdown on the migration and invasion ability of HGC-27 and MKN-45 cells were evaluated by Transwell migration and invasion assay. **L** After circHAS2 was knocked down, the expressions of N-cad and Vimentin, key proteins of EMT, were detected by Western blot. *** $P < 0.001$, **** $P < 0.0001$.

with RNase R and found that circHAS2 exhibited better antidigestion ability compared to linear HAS2 (Fig. 2E). In addition, after treatment with AGS and MKN-45 cells by actinomycin D, the stability of circHAS2 was stronger than that of linear HAS2 (Fig. 2F), further confirming the stability of the circular structure and indicating that circHAS2 had good stability. By comparing the expression levels of circHAS2 and its transcriptional gene HAS2 in 20 pairs of GC tissues and paired paracancerous tissues, it was found that only circHAS2 showed significant differential expression in GC tissues (Fig. 2G). These results demonstrate that the ring-like structure of circHAS2 may be a factor affecting the progression of GC.

CircHAS2 can promote the proliferation and metastasis of GC cells

To assess the effects of circHAS2 on cell proliferation, migration, and invasion during the progression of GC, we conducted in vitro

functional experiments. The expression of circHAS2 in GC cells was investigated by qPCR. As shown in Fig. 3A, the expression levels of circHAS2 in GC cells (SGC-7901, HGC-27, MKN-45, MKN-1, BGC-823, AGS) were all increased compared to GC epithelial cells. We knocked down circHAS2 expression (shRNA1 and shRNA2) in HGC-27 and MKN-45 cells (Fig. 3B). The CCK-8 assay and colony formation assay demonstrated that cell proliferation was significantly inhibited after circHAS2 knockdown compared to the control group (Fig. 3C–E). Similarly, the EdU assay further demonstrated that the number of proliferating cells was significantly reduced after circHAS2 knockdown (Fig. 3F and G). These experiments suggest that circHAS2 can promote the proliferation of GC cells. Subsequently, we used the transwell assay to investigate the migration and invasion ability of GC cells after circHAS2 knockdown. The transwell assay demonstrated that the migration and invasion abilities of HGC-27 and MKN-45 cells after circHAS2 knockdown were significantly reduced (Fig. 3H–K).

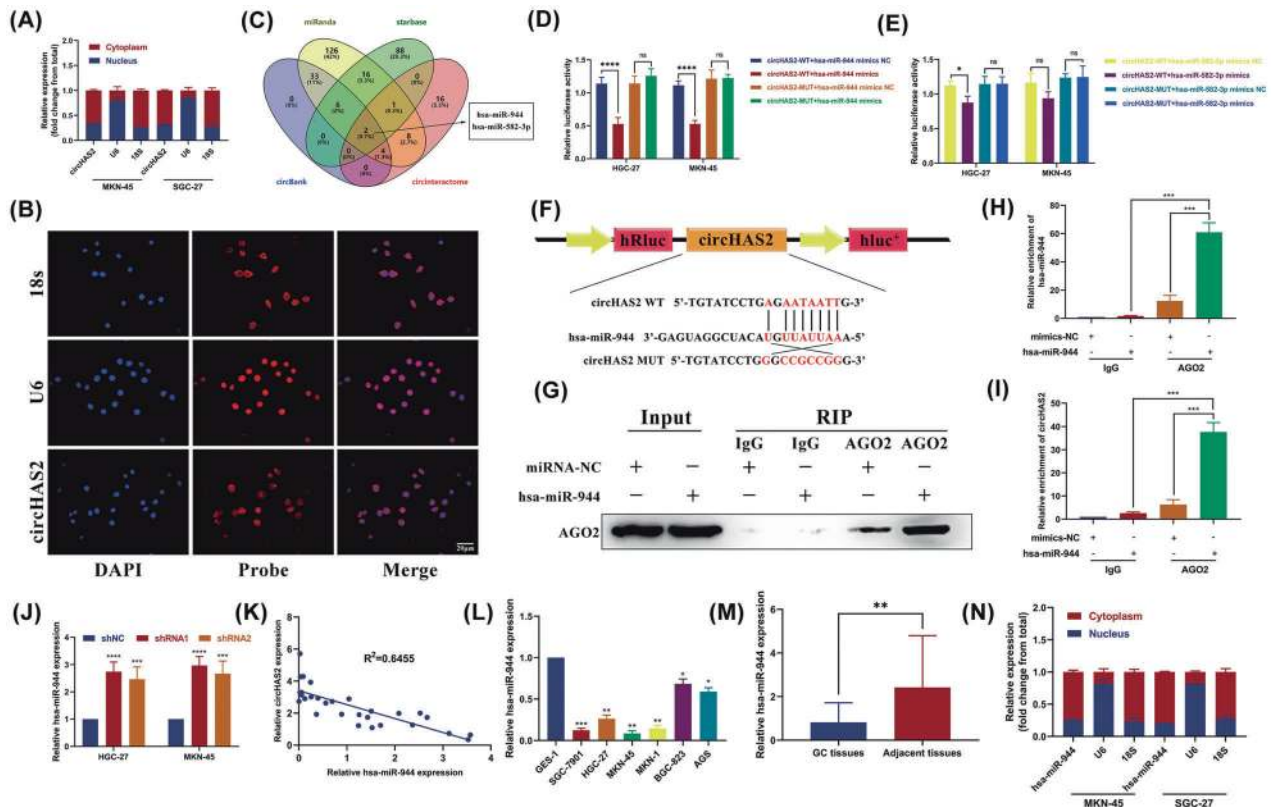


Fig. 4 Determination of hsa-miR-944 as the target gene of circHAS2. **A** and **B** The localization of circHAS2 in GC cells was determined by nucleoplasmic separation and FISH assay. **C** Prediction of downstream target genes for circHAS2 binding using bioinformatics websites. **D** and **E** The direct binding of circHAS2 to hsa-miR-944 was verified by dual luciferin no reporter gene assay. **F** Schematic diagram of binding sites between wild-type circHAS2 and hsa-miR-944. **G** Anti-AGO2 RIP analysis of the expression of AGO2 protein detected by western blotting. **H** and **I** Detection of circHAS2 and hsa-miR-944 by qPCR. **J** The expression level of hsa-miR-944 after circHAS2 knockdown in HGC-27 and MKN-45 cells. **K** The correlation between hsa-miR-944 and circHAS2 in GC was analyzed by Pearson correlation analysis. **L** The expression level of hsa-miR-944 in GC cells was detected by qPCR. **M** The expression level of hsa-miR-944 in GC tissues and adjacent tissues was detected by qPCR. **N** The localization of hsa-miR-944 in GC cells was confirmed by nucleoplasmic separation assay. * $P < 0.05$, ** $P < 0.01$, *** $P < 0.001$, **** $P < 0.0001$.

Western blot analysis showed that N-cadherin (N-cad) and vimentin expression in HGC-27 and MKN-45 cells was decreased after circHAS2 knockdown (Fig. 3L). To investigate the specific functional effects of circHAS2 on GC cells, we knocked down the expression of HAS2 in HGC-27 with MKN-45 cells and subsequently performed cellular assays. CCK-8, colony formation, and transwell assays demonstrated that knockdown of HAS2 had no effects on the proliferation, migration, and invasive abilities of GC cells (Supplementary Fig. 1). These results confirmed that circHAS2 promoted the proliferation, migration, and invasion of GC cells and was related to the epithelial-mesenchymal transition (EMT).

CircHAS2 regulates GC development by sponging hsa-miR-944

To evaluate the regulatory mechanism of circHAS2 in GC, nucleoplasmic separation and fluorescence in situ hybridization assays were used to confirm that circHAS2 is mainly located in the cytoplasm (Fig. 4A and B). CircRNAs present in the cytoplasm mainly act as miRNA sponges to play a regulatory role in tumors [26, 27]. Therefore, we hypothesized that circHAS2 may be the ceRNA of GC. Thus, we predicted that the miRNAs hsa-miR-944 and hsa-miR-582-3p bound to circHAS2 through cross-analysis of four prediction databases: circAtlas, Starbase, CircBank, and Circinteractome (Fig. 4C). Subsequently, we used the luciferase gene reporter assay to demonstrate that hsa-miR-944 mimics inhibited the luciferase activity of WT circHAS2, while the luciferase activity of MUT type did not change (Fig. 4D). The hsa-miR-582-3p mimic did not affect the luciferase activity of WT

and MUT circHAS2 (Fig. 4E). These experiments demonstrate that circHAS2 binds to hsa-miR-944 (Fig. 4F). The binding of circRNA to miRNA is dependent on AGO2, and the two interact through the action of AGO2 protein [28]. To further confirm the relationship between circHAS2 and hsa-miR-944 in GC cells, we performed anti-AGO2 RIP assays in MKN-45 cells. Compared with IgG, anti-AGO2 antibody effectively downregulated AGO2 in MKN-45 cells transfected with hsa-miR-944 mimics (Fig. 4G). qPCR verified that circHAS2 and hsa-miR-944 were more abundant in hsa-miR-944 mimic-transfected MKN-45 cells than in the miR-NC group (Fig. 4H and I). The expression of hsa-miR-944 was increased after knockdown of circHAS2 (Fig. 4J). In addition, there was a negative correlation between the expression of circHAS2 and hsa-miR-944 in 20 pairs of GC tissues (Fig. 4K), and the expression of hsa-miR-944 was downregulated in both GC tissues and GC cells (Fig. 4L and M), which was mainly distributed in the cytoplasm (Fig. 4N). Therefore, hsa-miR-944 might be the downstream target gene of circHAS2 in GC.

As a target gene of circHAS2, hsa-miR-944 can inhibit the proliferation, migration, and invasion of GC cells

The above experiments demonstrated that hsa-miR-944 can be downregulated in GC cells as a target gene of circHAS2. Thus, we hypothesized that hsa-miR-944 may inhibit the progression of GC. As shown in Fig. 5A–C, the proliferation ability of HGC-27 and MKN-45 cells with the addition of hsa-miR-944 mimics was inhibited, as shown by the CCK-8 and cell colony formation experiments. The EdU assay also demonstrated that the number

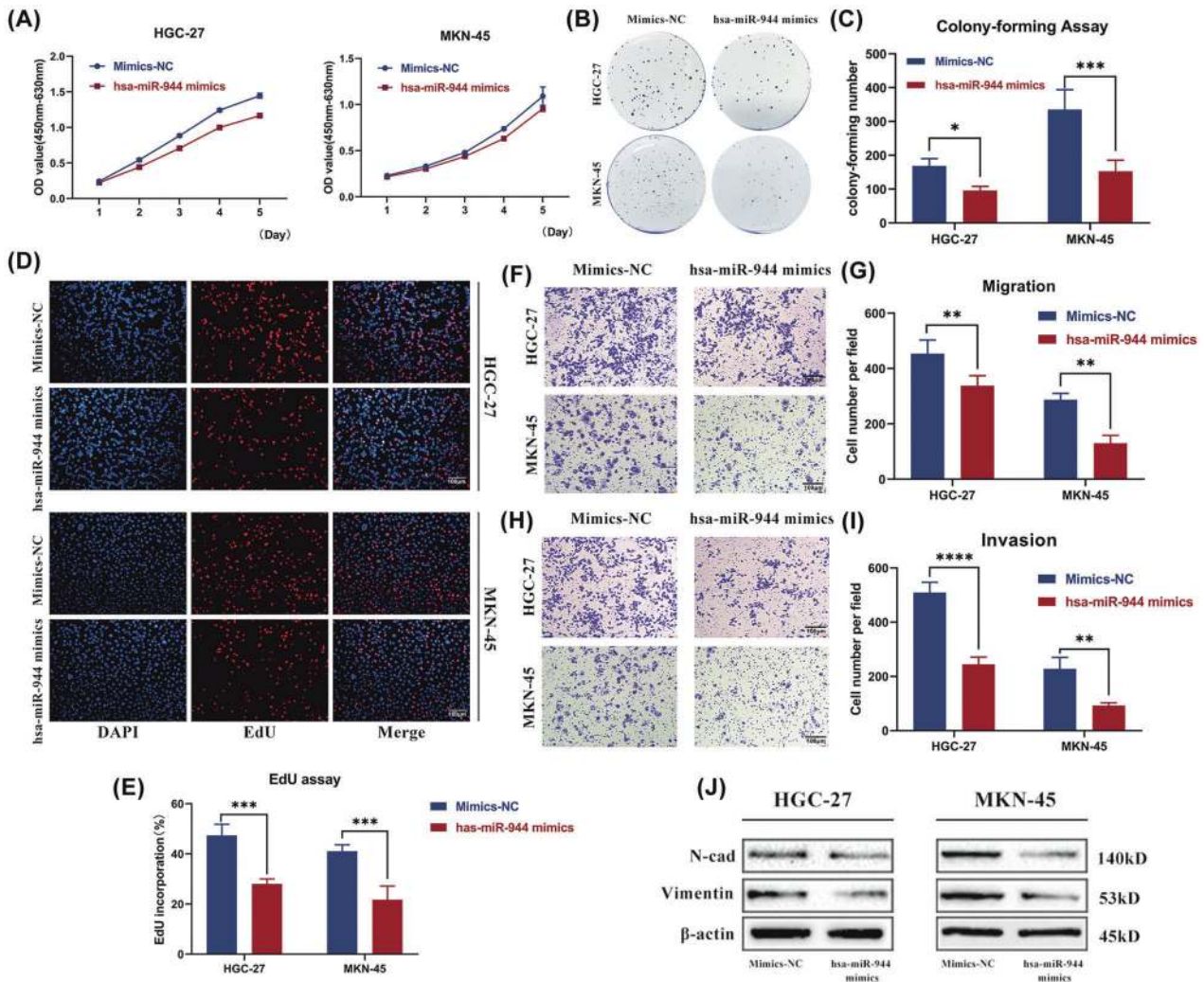


Fig. 5 Hsa-miR-944 can inhibit the proliferation, migration, and invasion of GC cells. **A–E** The effects of the addition of hsa-miR-944 mimics on the proliferation of HGC-27 and MKN-45 cells were evaluated by CCK-8, cell colony formation assay, and EdU assay. **F–I** The effects of the addition of hsa-miR-944 mimics on the migration and invasion ability of HGC-27 and MKN-45 cells were evaluated by Transwell migration and invasion assay. **J** After adding hsa-miR-944 mimics, the expressions of N-cad and Vimentin, key EMT proteins, were detected by Western blot. * $P < 0.05$, ** $P < 0.01$, *** $P < 0.001$, **** $P < 0.0001$.

of proliferating GC cells was significantly reduced after the addition of hsa-miR-944 mimics (Fig. 5D and E). The transwell assay demonstrated that HGC-27 and MKN-45 treated with hsa-miR-944 mimics had inhibited cell migration and invasion (Fig. 5F–I). Western blot analysis was used to detect the expression levels of key EMT proteins, and it was found that the expression of N-cadherin and vimentin in HGC-27 and MKN-45 cells treated with hsa-miR-944 mimics was decreased (Fig. 5J). These results suggest that as a target gene of circHAS2, hsa-miR-944 can inhibit the proliferation, migration, and invasion of GC cells.

As a target gene of hsa-miR-944, PPM1E is upregulated in GC
To further verify that circHAS2 may serve as a ceRNA in GC, we cross-analyzed the downstream target genes of hsa-miR-944 using the miRDB, miRWalk, miRpathDB, and TargetScan databases, and screened out eight mRNA molecules (Fig. 6A). To verify the binding relationship between these eight mRNAs and hsa-miR-944, only the expression of PPM1E was downregulated after the addition of hsa-miR-944 mimics to MKN-45 cells (Fig. 6B). Subsequently, we used luciferase gene reporter assays to confirm that the overexpression of hsa-miR-944 inhibited the luciferase activity of PPM1E, while MUT luciferase activity of PPM1E was not

affected (Fig. 6C and D). The results suggest that PPM1E might be the downstream target gene of hsa-miR-944. PPM1E expression was also reduced by circHAS2 knockdown in HGC-27 and MKN-45 cells (Fig. 6E). Western blot analysis also showed that PPM1E protein was significantly reduced after circHAS2 knockdown or the addition of hsa-miR-944 mimics, but the inhibitor of hsa-miR-944 rescued the inhibition of PPM1E expression after circHAS2 knockdown (Fig. 6F). In addition, the expression of PPM1E was upregulated in GC tissues and cells (Fig. 6G and H), and the expression of PPM1E was negatively correlated with the expression of hsa-miR-944 (Fig. 6I) and positively correlated with the expression of circHAS2 (Fig. 6J). These results indicate that the PPM1E gene can be used as a target gene of hsa-miR-944 and is induced by circHAS2 to upregulate the expression of PPM1E through sponging with hsa-miR-944.

Hsa-miR-944 specifically affects the growth, migration, or invasion of GC cells through PPM1E targeting

To determine whether hsa-miR-944 can affect the growth, migration, or invasion of GC cells specifically through PPM1E targeting, we added hsa-miR-944 mimics to HGC-27 and MKN-45 cells overexpressing PPM1E (Fig. 7A). The results of the CCK-8 and

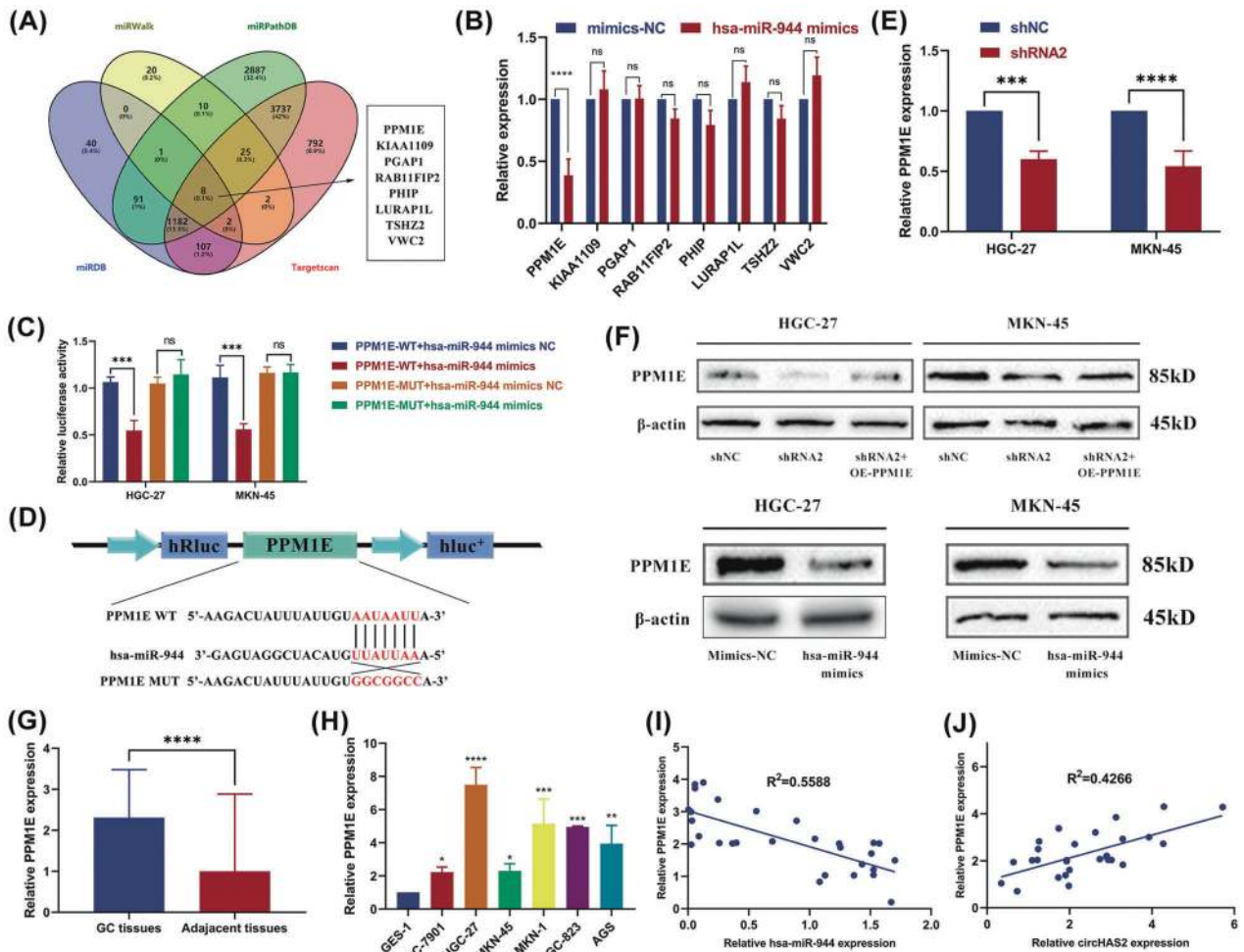


Fig. 6 circHAS2 regulates PPM1E through hsa-miR-944. **A** The downstream target genes of hsa-miR-944 binding were predicted using bioinformatics websites. **B** The expression of downstream target genes after the addition of hsa-miR-944 mimics was detected by qPCR. **C** The binding of hsa-miR-944 with PPM1E was verified by dual luciferin no reporter gene assay. **D** Schematic diagram of binding sites between wild-type PPM1E and hsa-miR-944. **E** The expression of PPM1E after circHAS2 knockdown was detected by qPCR. **F** The expression of PPM1E in HGC-27 and MKN-45 cells under different conditions was detected by Western Blot. **G** The expression level of PPM1E in GC tissues and paracancerous tissues was detected by qPCR. **H** The expression level of PPM1E in GC cells was detected by qPCR. **I–J** The correlation between PPM1E and circHAS2 and hsa-miR-944 in GC was analyzed by Pearson correlation analysis. * $P < 0.05$, ** $P < 0.01$, *** $P < 0.001$, **** $P < 0.0001$.

cell colony formation assays showed that the addition of hsa-miR-944 mimics rescued the proliferation of HGC-27 and MKN-45 cells overexpressing PPM1E (Fig. 7B–D). Meanwhile, the migration and invasion abilities of HGC-27 and MKN-45 cells overexpressing PPM1E were also rescued by adding hsa-miR-944 mimics as revealed by transwell assays (Fig. 7E–H). Western blot assays similarly demonstrated that the addition of hsa-miR-944 mimics rescued the proliferation effects on N-cadherin and vimentin after overexpression of PPM1E (Fig. 7I). These data suggest that hsa-miR-944 specifically affects the growth, migration, or invasion of GC cells through PPM1E targeting.

PPM1E can reverse the effects of circHAS2 knockdown on GC cells

To determine whether circHAS2 exerts its effects on GC through PPM1E, we restored PPM1E expression in circHAS2 knockdown HGC-27 and MKN-45 cells (Fig. 8A and B). The results of the CCK-8 and cell colony formation assays showed that PPM1E overexpression rescued the proliferation of circHAS2 knockdown HGC-27 and MKN-45 cells (Fig. 8C–E). At the same time, transwell experiments showed that the migration and invasion abilities of

circHAS2 knockdown HGC-27 and MKN-45 cells were also rescued after PPM1E overexpression (Fig. 8F–I). Western blot analysis also demonstrated that PPM1E overexpression rescued the inhibition of N-cadherin and vimentin after circHAS2 knockdown (Fig. 8J). These data suggest that circHAS2 can regulate GC progression through PPM1E.

DISCUSSION

GC is the third leading cause of death worldwide [1]. Although great progress has been made in the treatment of GC tissues, the recurrence rate is still very high due to the strong tumor heterogeneity [29, 30], so it is urgent to identify biomarkers with strong sensitivity and specificity. In recent years, with the development of high-throughput sequencing, many noncoding RNAs have emerged. Among them, circRNAs have a stable structure, tumor-specific, and long half-life. Simultaneously, circRNA can act as circRNAs and also serve as miRNA sponges, RNA-binding protein scaffolds, transcriptional regulators, and potential translation templates [31, 32]. Thus, circRNAs may serve as potential biomarkers and therapeutic targets for GC.

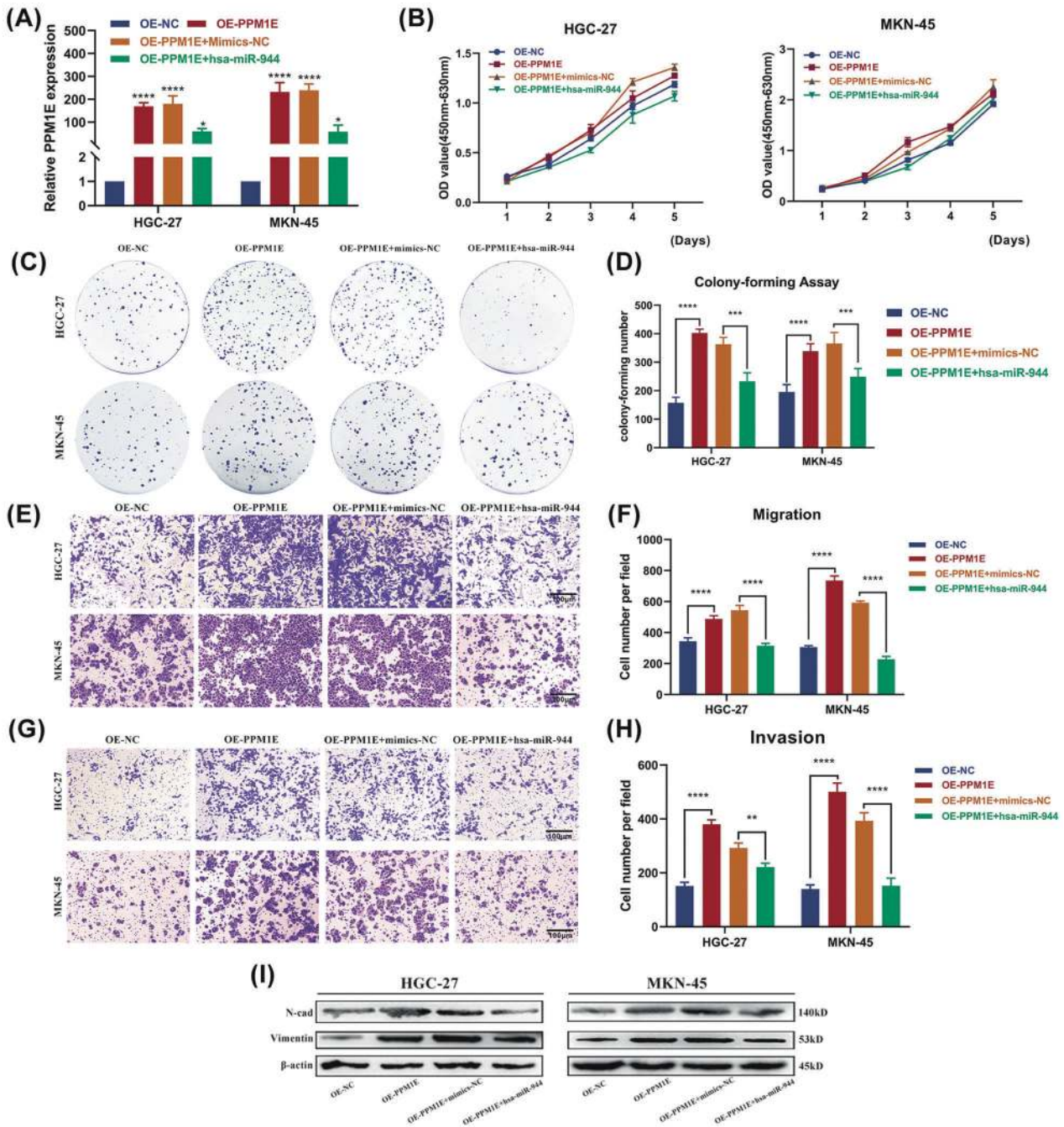


Fig. 7 has-miR-944 inhibits the proliferation, migration and invasion of gastric cancer by targeting PPM1E. **A–I** Transfection of OE-NC, OE-PPM1E, OE-PPM1E + mimics-NC, OE-PPM1E + mimics into HGC-27 and MKN-45 cells. **A** qPCR was performed to detect the expression level of PPM1E in HGC-27 and MKN-45 cells. **B–D** The effect on the proliferative capacity of HGC-27 and MKN-45 cells under different conditions was evaluated by CCK-8, cell colony formation assay. **E–H**. The effects on the migration and invasion ability of HGC-27 and MKN-45 cells under different conditions were evaluated by Transwell migration and invasion assays. **I** Western blot assay to assess the expression of key EMT proteins in HGC-27 and MKN-45 cells under different conditions. * $p < 0.05$, ** $p < 0.01$, *** $p < 0.001$, **** $p < 0.0001$.

In this study, three pairs of circRNAs of GSE121445 in the Gene Expression Omnibus database were analyzed for differential expression in GC tissues and corresponding paracancer tissues, and circHAS2 with the strongest correlation and upregulated expression in GC tissues was screened by qPCR. Subsequently, we found that the expression of circHAS2 increased with the degree of lymph node metastasis, and clinical data analyses showed that the expression of circHAS2 was correlated with T stage, TNM stage, lymph node metastasis, and nerve/vascular invasion. These studies suggest that circHAS2 can be good biomarker for GC.

Survival curve analysis suggested that circHAS2 might be a good prognostic marker for GC. To verify the potential mechanism of circHAS2 in GC, we analyzed the effects of circHAS2 on the proliferation, migration, and invasion of GC cells. In vitro experiments showed that circHAS2 knockdown significantly inhibited the proliferation, migration, and invasion of GC cells and may be related to the EMT.

An increasing number of studies have revealed the potential mechanism of action of circRNAs. As miRNA sponges, circRNAs play a regulatory role in tumors [14, 21, 33]. Because circHAS2

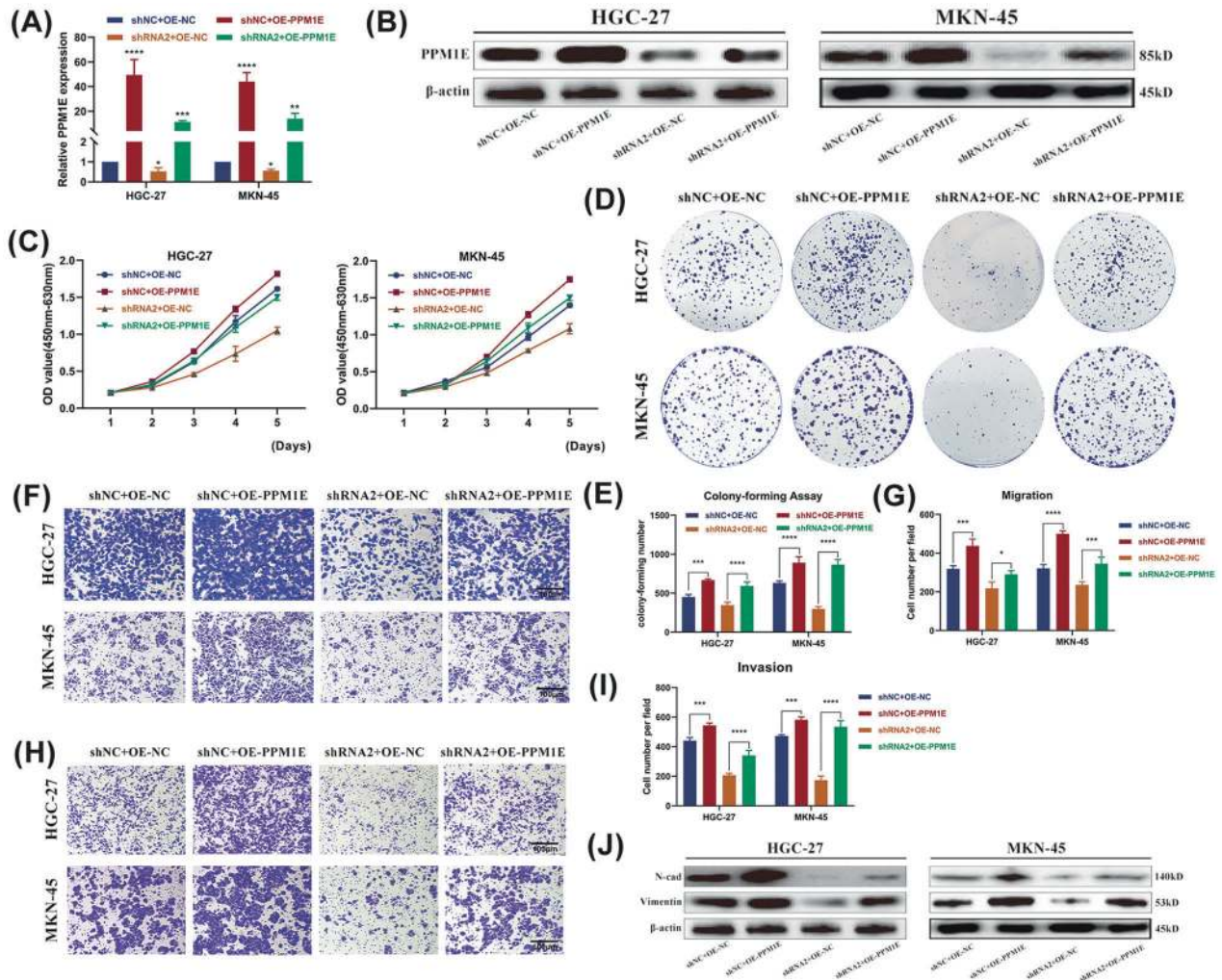


Fig. 8 PPM1E overexpression can reverse the inhibitory effect of circHAS2 knockdown on proliferation, migration, and invasion of GC cells. **A–J** shNC+OE-NC, shNC+OE-PPM1E, shRNA2+OE-NC, shRNA2+OE-PPM1E were transfected into HGC-27 and MKN-45 cells. **A** and **B** The expression level of PPM1E in HGC-27 and MKN-45 cells was detected by qPCR and Western blot. **C–E**. CCK-8 and cell colony formation experiments evaluated the effects of different conditions on the proliferation ability of HGC-27 and MKN-45 cells. **F–I** The effects of different conditions on the migration and invasion ability of HGC-27 and MKN-45 cells were evaluated by Transwell migration and invasion assay. **J** Western blot assay was used to evaluate the expression of key EMT proteins in HGC-27 and MKN-45 cells under different conditions. * $P < 0.05$, ** $P < 0.01$, *** $P < 0.001$, **** $P < 0.0001$.

mainly exists in the cytoplasm, it may regulate the development of GC through the competitive binding of miRNA. We verified that hsa-miR-944 is a potential target gene of circHAS2 using bioinformatics prediction websites and double fluorescence gene reporter experiments. In vitro experiments showed that the overexpression of hsa-miR-944 inhibited the proliferation, migration, and invasion of GC cells. These results suggest that circHAS2 may promote the development of GC by competitively binding with hsa-miR-944. Previous studies have shown that hsa-miR-944 plays a potential tumor-suppressive role in colorectal cancer through the ubiquitin-proteasome system [34]. In addition, Xi et al. [35] found that circCSPP1 knockdown attenuated adriamycin resistance and inhibited tumor progression in colorectal cancer via the miR-944 /FZD7 axis. Pan et al. [36] also found that the downregulated expression level of miR-944 in GC may prevent the EMT through the MACC1/MET/Akt signaling pathway, thereby inhibiting the metastasis of GC, and also confirming the mechanism and function of circRNA-miRNA in GC.

To study the downstream target genes of circHAS2-hsa-miR-944, further prediction and experiments showed that the mimics

of hsa-miR-944 can inhibit the luciferase activity of WT PPM1E. In addition, in vitro rescue experiments showed that hsa-miR-944 specifically affected the growth, migration, or invasion of GC cells through PPM1E targeting. These results suggest that hsa-miR-944 may regulate the progression of GC in combination with PPM1E. PPM1E is an AMP-activated protein kinase phosphatase [37]; PPM1E may induce AMPK activation, thus contributing to tumor progression. We found that the overexpression of hsa-miR-944 and knockdown of circHAS2 inhibited PPM1E mRNA and protein expression. The expression level of PPM1E was positively correlated with the expression level of circHAS2, and negatively correlated with the expression level of hsa-miR-944. Overexpression of PPM1E can restore the ability of circHAS2 knockdown to the proliferation, migration, and invasion of GC cells.

In summary, we identified a novel circRNA, circHAS2, which regulates PPM1E expression through hsa-miR-944. This axis plays a key role in regulating the occurrence and development of GC and provides a novel target for the treatment of GC, but the underlying mechanisms still need to be further explored.

REFERENCES

- Bray F, Ferlay J, Soerjomataram I, Siegel RL, Torre LA, Jemal A. Global cancer statistics 2018: GLOBOCAN estimates of incidence and mortality worldwide for 36 cancers in 185 countries. *CA Cancer J Clin.* 2018;68:394–424.
- Cheng J, Cai M, Shuai X, Gao J, Wang G, Tao K. Systemic therapy for previously treated advanced gastric cancer: A systematic review and network meta-analysis. *Crit Rev Oncol Hematol.* 2019;143:27–45.
- Smyth EC, Nilsson M, Grabsch HI, van Grieken NC, Lordick F. Gastric cancer. *Lancet.* 2020;396:635–48.
- Zhang LH, Wang Z, Li LH, Liu YK, Jin LF, Qi XW, et al. Vestigial like family member 3 is a novel prognostic biomarker for gastric cancer. *World J Clin cases.* 2019;7:1954–63.
- Valastyan S, Weinberg RA. Tumor metastasis: molecular insights and evolving paradigms. *Cell.* 2011;147:275–92.
- Allemani C, Weir HK, Carreira H, Harewood R, Spika D, Wang XS, et al. Global surveillance of cancer survival 1995–2009: analysis of individual data for 25,676,887 patients from 279 population-based registries in 67 countries (CONCORD-2). *Lancet.* 2015;385:977–1010.
- Ashwal-Fluss R, Meyer M, Pamudurti NR, Ivanov A, Bartok O, Hanan M, et al. circRNA biogenesis competes with pre-mRNA splicing. *Mol Cell.* 2014; 56:55–66.
- Qu S, Yang X, Li X, Wang J, Gao Y, Shang R, et al. Circular RNA: a new star of noncoding RNAs. *Cancer Lett.* 2015;365:141–8.
- Memczak S, Jens M, Elefsinioti A, Torti F, Krueger J, Rybak A, et al. Circular RNAs are a large class of animal RNAs with regulatory potency. *Nature.* 2013;495:333–8.
- Capel B, Swain A, Nicolis S, Hacker A, Walter M, Koopman P, et al. Circular transcripts of the testis-determining gene *Sry* in adult mouse testis. *Cell.* 1993;73:1019–30.
- Nigro JM, Cho KR, Fearon ER, Kern SE, Ruppert JM, Oliner JD, et al. Scrambled exons. *Cell.* 1991;64:607–13.
- Ma S, Kong S, Wang F, Ju S. CircRNAs: biogenesis, functions, and role in drug-resistant Tumours. *Mol Cancer.* 2020;19:119.
- Ding L, Zhao Y, Dang S, Wang Y, Li X, Yu X, et al. Circular RNA circ-DONSON facilitates gastric cancer growth and invasion via NURF complex dependent activation of transcription factor SOX4. *Mol Cancer.* 2019;18:45.
- Fan Y, Wang J, Jin W, Sun Y, Xu Y, Wang Y, et al. CircNR3C2 promotes HRD1-mediated tumor-suppressive effect via sponging miR-513a-3p in triple-negative breast cancer. *Mol Cancer.* 2021;20:25.
- Zhang M, Zhao K, Xu X, Yang Y, Yan S, Wei P, et al. A peptide encoded by circular form of LINC-PINT suppresses oncogenic transcriptional elongation in glioblastoma. *Nat Commun.* 2018;9:4475.
- Gross JD, Moerke NJ, von der Haar T, Lugovskoy AA, Sachs AB, McCarthy JE, et al. Ribosome loading onto the mRNA cap is driven by conformational coupling between eIF4G and eIF4E. *Cell.* 2003;115:739–50.
- Godet AC, David F, Hantelys F, Tatin F, Lacazette E, Garmy-Susini B, et al. IRES trans-acting factors, key actors of the stress response. *Int J Mol Sci.* 2019;20:924.
- Hansen TB, Jensen TI, Clausen BH, Bramsen JB, Finsen B, Damgaard CK, et al. Natural RNA circles function as efficient microRNA sponges. *Nature.* 2013;495:384–8.
- Zhao Z, Ji M, Wang Q, He N, Li Y. Circular RNA Cdr1as upregulates SCAL to suppress cisplatin resistance in ovarian cancer via miR-1270 suppression. *Molecular therapy. Nucleic acids.* 2019;18:24–33.
- Zhong Z, Lv M, Chen J. Screening differential circular RNA expression profiles reveals the regulatory role of circTCF25-miR-103a-3p/miR-107-CDK6 pathway in bladder carcinoma. *Sci Rep.* 2016;6:30919.
- Peng L, Sang H, Wei S, Li Y, Jin D, Zhu X, et al. circCUL2 regulates gastric cancer malignant transformation and cisplatin resistance by modulating autophagy activation via miR-142-3p/ROCK2. *Mol Cancer.* 2020;19:156.
- Ma W, Xue N, Zhang J, Wang D, Yao X, Lin L, et al. circUBAP2 regulates osteosarcoma progression via the miR-204-3p/HMGA2 axis. *Int J Oncol.* 2021;58:298–311.
- Lv Q, Wang G, Zhang Y, Shen A, Tang J, Sun Y, et al. CircAGAP1 promotes tumor progression by sponging miR-15-5p in clear cell renal cell carcinoma. *J Exp Clin cancer Res: CR.* 2021;40:76.
- Ma S, Kong S, Gu X, Xu Y, Tao M, Shen L, et al. As a biomarker for gastric cancer, circPTPN22 regulates the progression of gastric cancer through the EMT pathway. *Cancer cell Int.* 2021;21:44.
- Wang H, Wang N, Zheng X, Wu L, Fan C, Li X, et al. Circular RNA hsa_circ_0009172 suppresses gastric cancer by regulation of microRNA-485-3p-mediated NTRK3. *Cancer Gene Ther.* 2021;1:131.
- Cao J, Zhang X, Xu P, Wang H, Wang S, Zhang L, et al. Circular RNA circLMO7 acts as a microRNA-30a-3p sponge to promote gastric cancer progression via the WNT2/β-catenin pathway. *J Exp Clin Cancer Res: CR.* 2021;40:6.
- Guo X, Dai X, Liu J, Cheng A, Qin C, Wang Z. Circular RNA circREPS2 Acts as a Sponge of miR-558 to Suppress Gastric Cancer Progression by Regulating RUNX3/β-catenin Signaling. *Molecular therapy. Nucleic Acids.* 2020;21:577–91.
- Patop IL, Wüst S, Kadener S. Past, present, and future of circRNAs. *EMBO J.* 2019;38:e100836.
- Lai SW, Kuo YH, Liao KF. Statin therapy and gastric cancer death. *Postgrad Med J.* 2020;96:178.
- Xu J, Zhang Z, Chen Q, Yang L, Yin J. miR-146b Regulates Cell Proliferation and Apoptosis in Gastric Cancer by Targeting PTP1B. *Digestive Dis Sci.* 2020;65:457–63.
- Shan C, Zhang Y, Hao X, Gao J, Chen X, Wang K. Biogenesis, functions and clinical significance of circRNAs in gastric cancer. *Mol Cancer.* 2019;18:136.
- Chen LL. The expanding regulatory mechanisms and cellular functions of circular RNAs. *Nat Rev Mol Cell Biol.* 2020;21:475–90.
- Yu Z, Zhu X, Li Y, Liang M, Liu M, Liu Z, et al. Circ-HMGA2 (hsa_circ_0027446) promotes the metastasis and epithelial-mesenchymal transition of lung adenocarcinoma cells through the miR-1236-3p/ZEB1 axis. *Cell death Dis.* 2021;12:313.
- Shan YJ, Lee JH, Jin S, Kim JH, Kim SH. Primate-specific miR-944 activates p53-dependent tumor suppression in human colorectal cancers. *Cancer Lett.* 2019;440–41:168–79.
- Xi L, Liu Q, Zhang W, Luo L, Song J, Liu R, et al. Circular RNA circCSPP1 knockdown attenuates doxorubicin resistance and suppresses tumor progression of colorectal cancer via miR-944/FZD7 axis. *Cancer cell Int.* 2021;21:153.
- Pan T, Chen W, Yuan X, Shen J, Qin C, Wang L. miR-944 inhibits metastasis of gastric cancer by preventing the epithelial-mesenchymal transition via MACC1/Met/AKT signaling. *FEBS Open bio.* 2017;7:905–14.
- Voss M, Paterson J, Kellsall IR, Martin-Granados C, Hastie CJ, Peggie MW, et al. Ppm1E is an in cellulose AMP-activated protein kinase phosphatase. *Cell Signal.* 2011;23:114–24.

ACKNOWLEDGEMENTS

We appreciate all patients implicated in this study and thank all individuals contributed to this study. This project was supported by the National Natural Science Foundation of China (No.81871720, 82072363) and Nantong Technology Projects [grant number JC2018011, JC2019121]

AUTHOR CONTRIBUTIONS

S.M. and X.L.G. drafted and revised the paper, designed the experiment, and selected the topic. L.S., Y.H.C., and C.Q. participated in the revision of the paper. X.J.S. and S.Q.J. provided resources and guidance for the paper. All authors read and approved the final manuscript.

COMPETING INTERESTS

The authors declare no competing interests.

ETHICS STATEMENT

The datasets used and/or analyzed during the current study are available from the corresponding author on reasonable request. Ethics statement The ethics committee of the local hospital (ethical review report number: 2018-L055) approved the study.

ADDITIONAL INFORMATION

Supplementary information The online version contains supplementary material available at <https://doi.org/10.1038/s41419-021-04158-w>.

Correspondence and requests for materials should be addressed to Xianjuan Shen or Shaoqing Ju.

Reprints and permission information is available at <http://www.nature.com/reprints>

Publisher's note Springer Nature remains neutral with regard to jurisdictional claims in published maps and institutional affiliations.



Open Access This article is licensed under a Creative Commons Attribution 4.0 International License, which permits use, sharing, adaptation, distribution and reproduction in any medium or format, as long as you give appropriate credit to the original author(s) and the source, provide a link to the Creative Commons license, and indicate if changes were made. The images or other third party material in this article are included in the article's Creative Commons license, unless indicated otherwise in a credit line to the material. If material is not included in the

article's Creative Commons license and your intended use is not permitted by statutory regulation or exceeds the permitted use, you will need to obtain permission directly from the copyright holder. To view a copy of this license, visit <http://creativecommons.org/licenses/by/4.0/>.

© The Author(s) 2021